

Quantum dynamics of X<sub>2</sub>BC van der Waals clusters

Stephen K. Gray

ANL/CHM/CP--78499

Theoretical Chemistry Group, Chemistry Division  
Argonne National Laboratory, Argonne, IL 60439

DE93 006416

ABSTRACT

Wave packet calculations modeling vibrational predissociation in X<sub>2</sub>BC(v') van der Waals clusters are discussed. A model involving three active degrees of freedom is used. Cluster lifetimes and BC vibrational product distributions are obtained, and compared with available experimental results for He<sub>2</sub>Cl<sub>2</sub>, and Ne<sub>2</sub>Cl<sub>2</sub>. Some preliminary results for He<sub>2</sub>I<sub>2</sub> and Ne<sub>2</sub>I<sub>2</sub> are also discussed. Mechanistic issues, including the role of direct versus sequential mechanisms in leading to the production of 2X + BC are addressed, as well as the role of intramolecular vibrational relaxation (IVR). Higher dimension extensions of the model are suggested.

1. INTRODUCTION

The spectroscopy and dynamics of XBC van der Waals (vdW) complexes, where X is a noble gas atom and BC denotes a halogen molecule, have been extensively studied experimentally with the aid of supersonic jets and modern laser technology.<sup>1-7</sup> Often pairwise interactions are an adequate description of the potential energy, and relatively few BC internal vibrational states are involved in the dynamics. Therefore reasonable empirical potential surfaces can be devised, and accurate quantum dynamics calculations can be performed. It is extremely rare in chemistry for this to be the case! Thus XBC systems offer unique opportunities for comparison of theory and experiment, and for studying certain dynamical effects, such as interference effects,<sup>2,3,5</sup> and the role of intramolecular vibrational relaxation (IVR).<sup>1,6,7</sup> Such effects are important in dynamics of covalently bonded systems, but are often difficult to isolate or study in any unambiguous manner. The larger vdW clusters X<sub>n</sub>BC, with n > 1, have also been of interest.<sup>8-18</sup> Even for small n, the X<sub>n</sub>BC systems can offer a much richer dynamics than XBC systems. Unfortunately, theoretical calculations become significantly more difficult when four or more atoms are involved. In this paper I review recent wave packet calculations<sup>18</sup> that model vibrational predissociation of the n = 2 clusters,

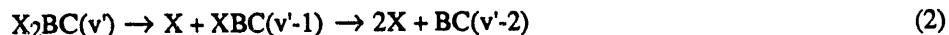


corresponding to He<sub>2</sub>Cl<sub>2</sub> and Ne<sub>2</sub>Cl<sub>2</sub>, and also present some preliminary results for He<sub>2</sub>I<sub>2</sub> and Ne<sub>2</sub>I<sub>2</sub>. The theoretical results are contrasted with available experimental results.<sup>8-11,17</sup> Experiments typically involve creation of ground electronic and vibrational state complexes in a supersonic jet and optical laser excitation to "pump" an electronically excited state (the "B" state). The pump frequency is chosen such that X<sub>2</sub>BC on the B state has, effectively, v' quanta of excitation in BC, and zero-point energy in the vdW modes. The fragmentation dynamics is determined exclusively by motion on the B state, although it is common to probe this dynamics via absorption and or emission to other electronic states. Early experimental work relied on spontaneous emission,<sup>8,9</sup> whereas more recent work<sup>10,11,17</sup> has employed stimulated emission and absorption via application of a second "probe" laser pulse. Real-time experiments, wherein pump-probe techniques are used to map out product populations as a function of time have also been performed on some XBC and X<sub>2</sub>BC systems.<sup>4,17</sup>

It is worthwhile to outline dynamical issues that arise in the X<sub>n</sub>BC systems of interest. The initial vibrational excitations v' in BC are usually sufficiently large, and the dynamics is generally dominated by relatively small vibrational quantum number differences v' - v<sub>F</sub>. This means that no appreciable amounts of X + XBC(v) products can occur, because the triatomic complexes XBC(v) are all metastable and eventually decay to X + BC. It is possible to form X<sub>2</sub> + BC products, although experimental and theoretical evidence suggest that this channel is not extremely important. Levi's group has carried out pioneering work<sup>8,9</sup> on the He<sub>2</sub>I<sub>2</sub> and Ne<sub>2</sub>I<sub>2</sub> systems, among many others. In the case of He<sub>2</sub>I<sub>2</sub>(v'=22), the v<sub>F</sub> = v'-1 product channel is most likely open, i.e. the energy difference between v' and v'-1 BC vibrational states is greater than the energy required to expel both He atoms, but the primary I<sub>2</sub> products observed are in v<sub>F</sub> = v'-2. This and other evidence led Levi and co-workers to suggest that a sequential mechanism

MASTER

The submitted manuscript has been authored by a contractor of the U. S. Government under contract No. W-31-109-ENG-38. Accordingly, the U. S. Government retains a nonexclusive, royalty-free license to publish or reproduce the published form of this contribution, or allow others to do so, for U. S. Government purposes.



is operative, and that there is little correlation between departure of each  $X = \text{He}$  atom. They observed a different situation for  $\text{Ne}_2\text{I}_2(v'=21 \text{ or } 22)$ , with significant amounts of  $v'-3$  product being present in addition to  $v'-2$  products. (The  $v_f = v'-1$  channel is closed for  $\text{Ne}_2\text{I}_2$  at these levels of  $v'$  excitation.) This suggested a more complex dynamics occurs with  $\text{Ne}_2\text{I}_2$ , with more correlation between the two Ne atoms. Recent real-time experiments from Zewail's group<sup>17</sup> have in fact suggested that IVR effects may be present in  $\text{Ne}_2\text{I}_2$ , e.g. that certain internally excited intermediates may have to be invoked to fully understand the dynamics. Janda's group has carried out experimental studies<sup>10,11</sup> on  $\text{He}_2\text{Cl}_2$  and  $\text{Ne}_2\text{Cl}_2$ . It was shown that  $\text{He}_2\text{Cl}_2$  is extremely floppy and perhaps already in a kind of "quantum liquid" limit. Some aspects of the  $\text{He}_2\text{Cl}_2$  vibrational predissociation dynamics were also revealed: as with the earlier  $\text{He}_2\text{I}_2$  work, almost all the BC products corresponded to  $v_f = v'-2$ , consistent with a sequential fragmentation mechanism in the excitation range  $8 \leq v' \leq 13$  studied. A similar excitation range was studied in  $\text{Ne}_2\text{Cl}_2$ , and for the lower  $v'$  excitations both  $v'-1$  and  $v'-2$  products were observed, consistent with competition between direct and sequential mechanisms. As  $v'$  increases, the  $v'-1$  channel closes, and only  $v'-2$  products are seen. These results again point to  $X = \text{Ne}$  systems being more dynamically complex than the  $X = \text{He}$  case, although in  $\text{Ne}_2\text{Cl}_2$ , at least for the  $v'$  excitations examined, there were no signs of IVR effects.

Section 2 below presents the theoretical model and computational details. Sec. 3 discusses results obtained by Le Quere and Gray<sup>18</sup> for  $\text{He}_2\text{Cl}_2$  and  $\text{Ne}_2\text{Cl}_2$ , and Sec. 4 presents preliminary results for  $\text{He}_2\text{I}_2$  and  $\text{Ne}_2\text{I}_2$ . Sec. 5 summarizes.

## 2. THE MODEL AND COMPUTATIONAL DETAILS

### 2.1 A three degrees of freedom model

It is not practical, for the cases of interest here, to carry out full dimensional wave packet calculations. Instead, a reduced dimension model involving three degrees of freedom is employed, as schematically outlined in Fig. 1. The active degrees of freedom are  $R_1 =$  distance of one noble gas atom to the center of mass of BC,  $R_2 =$  distance of the other noble gas atom to the center of mass of BC, and  $r$ , the BC internuclear distance. The X atoms are restricted to motion within a plane perpendicular to and passing through the BC center of mass and the angle  $\theta$  between the  $R_1$  and  $R_2$  vdW bonds is taken to be fixed. The main advantage of this model is that  $2X + BC$  and  $X + XBC$  continua are easily identified and treated. Thus, mechanistic issues involving direct and sequential mechanisms can be addressed. Similar models (but with less restrictions) have been used by Villarreal and co-workers in approximate quantum and quasiclassical trajectory work.<sup>13-15</sup>

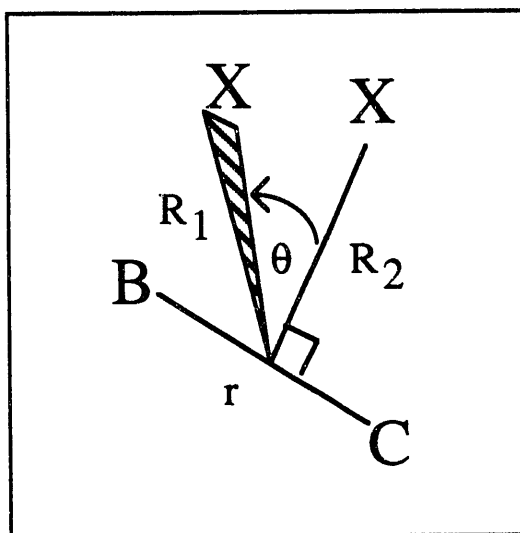


Fig. 1 Schematic diagram of the model. The active variables are  $R_1$ ,  $R_2$  and  $r$ , with  $\theta$  held fixed at an appropriate equilibrium value.

A reasonable Hamiltonian to employ is:

$$H = \frac{(P_1^2 + P_2^2)}{2\mu} + \frac{\cos\theta P_1 P_2}{(m_B + m_C)} + \frac{p^2}{2m} + V(R_1, R_2, r; \theta) , \quad (3)$$

with masses  $\mu = m_X(m_B + m_C)/(m_X + m_B + m_C)$ ,  $m = m_B m_C / (m_B + m_C)$ .  $P_1$ ,  $P_2$ , and  $p$  are momentum operators associated with the coordinates  $R_1$ ,  $R_2$ , and  $r$ , respectively. Eq. (3) is a simple generalization of the local mode Hamiltonian employed in studies of triatomic molecules.<sup>19</sup>

The potential (associated with the B electronic state) is assumed to be a sum of atom-atom Morse interactions,

$$V(R_1, R_2, r) = \sum_{ab} V_{ab}(R_{ab}) , \quad (4a)$$

$$V(R_{ab}) = D_{ab} [z^2 - 2z] , \quad z = \exp[-\alpha_{ab}(R_{ab} - R_{ab}^e)] , \quad (4b)$$

with the  $R_{ab}$  being functions of  $R_1$ ,  $R_2$ ,  $r$  (and depending parametrically on  $\theta$ ) as determined in a straightforward manner by the geometry of the model. The equilibrium value  $\theta \approx 50^\circ$  is used for all four  $X_2BC$  systems. The relevant Morse parameters are presented in Table 1.

Table 1. Atom-atom Morse potential interactions<sup>(a)</sup>

ab	$D_{ab}/\text{cm}^{-1}$	$\alpha_{ab}/\text{a.u.}$	$R_{ab}^e/\text{a.u.}$
Cl <sub>2</sub>	3145	1.245	4.5612
I <sub>2</sub>	4600.	0.9583	5.6955
HeCl	14	0.8467	6.8030
NeCl	39	0.9525	6.9920
HeI	18.	0.6033	7.5589
NeI	42.5	0.8100	7.5589
He <sub>2</sub>	7.61	1.1250	5.5993
Ne <sub>2</sub>	29.4	1.1049	5.8412

(a) Cl<sub>2</sub> and XCl parameters from Ref. [5]; I<sub>2</sub> parameters from Ref. [7]; He<sub>2</sub> parameters from Ref. [14]; Ne<sub>2</sub> parameters from Ref. [15]; HeI parameters from Ref. [20]. The NeI parameters have been chosen to describe the spectroscopy and dynamics<sup>4</sup> of NeI<sub>2</sub>.

## 2.2 Metastable states, propagation, and absorption

The coordinate space representation of the Hamiltonian operator Eq. (1) is obtained with the replacements  $P_i = -i\hbar \partial / \partial R_i$  and  $p = -i\hbar \partial / \partial r$ , and the time-dependent Schrödinger equation is given by

$$\frac{\partial}{\partial t} \Psi(R_1, R_2, r, t) = -\frac{iH}{\hbar} \Psi(R_1, R_2, r, t) , \quad (5)$$

with  $|\Psi(R_1, R_2, r, t)|^2 dR_1 dR_2 dr$  being interpreted as the probability the system is within the volume element  $(dR_1, dR_2, dr)$  about  $(R_1, R_2, r)$  at time  $t$ . It is necessary to specify an initial condition  $\Psi(t=0)$  and to solve Eq. (5) subject to this condition, i.e. to propagate  $\Psi(0)$  in time.

The initial conditions are chosen to be metastable states obtained by carrying out a *small* diagonalization of  $H$  in a bound state basis. A similar procedure has been employed in XBC wave packet work.<sup>5,7</sup> Let  $\langle r | v \rangle = \chi_v(r)$  denote a set of BC Morse oscillator vibration states, and  $\langle R_1, R_2 | n_1, n_2 \rangle = \phi_{n_1}(R_1) \phi_{n_2}(R_2)$  denote a set of zero-order vdW stretching states. (Harmonic oscillator states are used for the vdW stretches in these calculations.) Diagonalization of the vibrationally adiabatic Hamiltonian  $H_{v'} = \langle v=v' | H | v=v' \rangle$  in the  $|n_1, n_2\rangle$  basis, i.e. diagonalization of  $\langle n_1, n_2 | H_{v'} | n_1, n_2 \rangle$  leads to a set of vdW stretching states associated with  $v = v'$ . The metastable state that corresponds to  $v = v'$  quanta of excitation in BC and zero-point in the vdW stretches, the lowest vdW state in the  $v'$  manifold, is the particular metastable state that is propagated, since it corresponds to the kind of state assessed in experiments. Small Hamiltonian matrices, typically of dimension 25 by 25 are suitable for the determination of this metastable state.

Propagation is carried out in a stepwise fashion, and may be denoted as:

$$\Psi[k\tau] = \exp(-iH\tau / \hbar) \Psi[(k-1)\tau] \quad , \quad k = 1, 2, \dots \quad (6)$$

with  $\tau$  being a suitable time step. The major computational effort lies in evaluating the exponential operator in Eq. (6). A Lanczos procedure is used.<sup>21</sup> This can be thought of as involving, per time step,  $M$  acts of the Hamiltonian operator on the current wave packet, which effectively allows an accurate representation of the exponential operator (over the time interval of interest) to be constructed. Actually, I employ two iterative equations for the real and imaginary parts of the wave packet that are completely equivalent to Eq. (6), and use the Lanczos procedure to evaluate the operator actions in these two equations. This procedure is twice as efficient as applying the Lanczos method directly to Eq. (6). See Ref. [21] for details. Typically,  $\tau \approx 10$  fs, and  $M = 15$  in this work, and propagations of duration not more than 30 ps are adequate for inferring all relevant quantities. The structure of the problem is such that the wave packet is most conveniently expanded as

$$\Psi(R_1, R_2, r, t) = \sum_v C_v(R_1, R_2, t) \chi_v(r) \quad , \quad (7)$$

where the sum is restricted to a small number of BC vibrational states. Three vibrational states ( $v = v', v'-1, v'-2, v'-3$ ) are found to be adequate when relatively low initial excitations  $v' \leq 13$  are studied, and four ( $v = v', v'-1, v'-2, v'-3, v'-4$ ) vibrational states are suitable for calculations in the range  $14 \leq v' \leq 21$ . An evenly spaced square grid in  $R_1$  and  $R_2$  is employed, with each vdW bond vector being given by  $R_0 + (i-1) \Delta R$ ,  $i = 1, 2, \dots, N_R$ . Typical grid parameters are those employed in the  $\text{Ne}_2\text{Cl}_2$  calculations:  $\Delta R = 0.25$  a.u.,  $N_R = 128$ , and  $R_0 = 4$  a.u. Depending on the  $\text{X}_2\text{BC}$  system studied, slightly different  $R_0$  and  $\Delta R$  values must be employed owing to small differences in potential ranges.

Unfortunately, wave packet amplitude can approach the borders of the  $(R_1, R_2)$  grid. When this happens, it can be reflected back into the interaction region and thus lead to errors. To minimize such artificial reflection effects it is necessary to absorb wave packet amplitude. A convenient approach, which has proved adequate in earlier studies of XBC vdW systems,<sup>5,7</sup> is to absorb the  $C_v$  amplitudes according to:

$$C_v^a(R_1, R_2, t) = a(R_1) a(R_2) C_v(R_1, R_2, t) \quad , \quad (8a)$$

with

$$a(R_i) = \begin{cases} \exp[-\alpha(R_i - R_a)^2] & , \quad R_a \leq R_i \leq R_m \\ 1 & , \quad R_i < R_a \end{cases} \quad (8b)$$

$R_m = R_0 + (N_R - 1) \Delta R$  is the maximum  $R_1$  or  $R_2$  grid point, and Eq. (8) corresponds to reducing wave packet amplitude between  $R_a$  and  $R_m$  along both vdW bonds. It is not necessary to absorb every time step  $\tau$ . A natural time scale to absorb is provided by the classical vibrational period  $\tau_{\text{vib}}(v')$  of a BC molecule in vibrational state  $v'$ . Typically,  $\tau_{\text{vib}}(v')$  ranges between 0.2 to 0.4 ps. Thus, Eq. (8) is applied every  $\tau_{\text{vib}}(v') / \tau \approx 30$  time steps. It is necessary to verify that the parameters used to define absorption ( $R_a$  and  $\alpha$ ) do not significantly alter the observed dynamics (e.g., calculated lifetimes and product distributions). Typical absorption parameters are those used for  $\text{Ne}_2\text{Cl}_2$ ,  $R_a = 20$  a.u. and  $\alpha = 0.2$  a.u.

### 2.3 Resonance energies, lifetimes, and product distributions

The wave packet correlation function,  $S(t) = \langle \Psi(0) | \Psi(t) \rangle$ , can easily be computed, and when properly analyzed leads to the resonance energies and lifetimes of interest. In fact, even if the duration of the propagation is less than a typical lifetime, it can sometimes be possible to extract out the relevant information. The basic idea is to fit  $S(t)$  to resonance form,

$$S_{\text{res}}(t) = \sum_{\text{res}} b_{\text{res}} \exp[-i(E_{\text{res}} - i\Gamma_{\text{res}}/2)t/\hbar] , \quad (9)$$

where  $b_{\text{res}}$ ,  $E_{\text{res}}$ , and  $\Gamma_{\text{res}}$  are considered to be fitting parameters. Actually, as stated this is a very difficult nonlinear least squares problem. However, I have recently shown<sup>21</sup> that a rather old method of spectral analysis known as Prony's method is ideally suited to this problem. Prony's method reduces the nonlinear least squares problem to two (sub-optimal) least squares problems, and leads to stable results. When metastable states are employed as initial conditions so that one, or at most a few resonances dominate the correlation function, excellent estimates of the resonance parameters result. In the present calculations, for example, propagations of duration one quarter or less of a typical lifetime ( $\hbar/\Gamma_{\text{res}}$ ) have been found to be adequate.

In XBC vibrational predissociation problems, the product distributions associated with internal BC product states can be computed in a relatively straightforward manner.<sup>5</sup> Unfortunately, difficulties arise with the corresponding  $X_2BC$  problem. For simplicity, I restrict attention to the overall wave packet probability distribution, i.e. no attempt to construct energy resolved probabilities is made. Actually, because of the relatively narrow spreads of the wave packets, typically much less than resonance energy spacings, there is not much difference between these probabilities and energy-resolved ones. Imagine dividing the  $(R_1, R_2)$  configuration space up into the regions I, P and C as indicated in Fig. 2. Region I is a general interaction region associated with  $X_2BC$  complexes; region C corresponds to configurations more appropriately termed  $X + XBC$  complexes, with one vdW bond significantly larger than the other; region P corresponds to the  $2X + BC$  product region. The parameters  $R_0$ ,  $R_a$ , and  $R_m$  are defined by the grid and absorption properties discussed in Sec. 2.2. The parameter  $R_c$  is taken to be about 2 a.u. greater than the last classical outer turning point associated with the highest lying XBC vdW stretching state. For  $\text{Ne}_2\text{Cl}_2$ ,  $R_c = 15$  a.u.

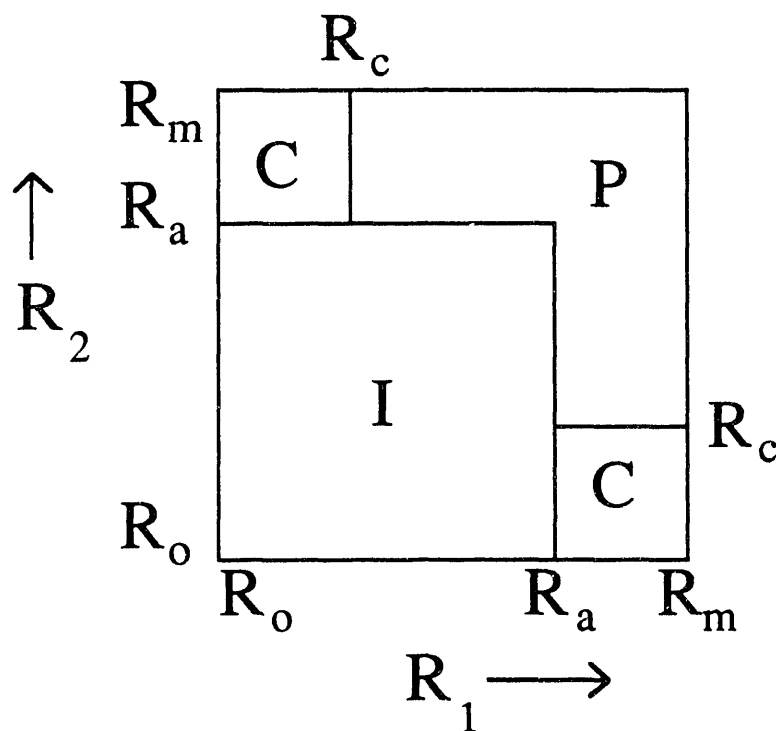


Fig. 2. Schematic diagram of the grids used to define the interaction region (I),  $X + XBC$  complex region (C), and  $2X + BC$  product region (P).

It is relatively easy to define vibrational state probabilities  $P_v^D$  associated with the D regions. One could imagine integrating the wave packet flux that crosses the relevant boundaries indicated in Fig. 2. Alternatively, one could explicitly accumulate vibrational state probability inside the D regions, allowing for the fact that some probability is absorbed every  $\tau_{\text{vib}}(v')$  time units. As shown in Ref. [22], a suitable expression for  $P_v^D(t)$  is:

$$P_v^D(t_n) = \langle C_v^a(t_n) | C_v^a(t_n) \rangle_D + \sum_{j=1}^n \left\{ \langle C_v(t_j) - C_v^a(t_j) | C_v(t_j) - C_v^a(t_j) \rangle_D + 2 \text{Re} \langle C_v^a(t_j) | C_v(t_j) - C_v^a(t_j) \rangle_D \right\}, \quad (10)$$

where  $D = I, P, \text{ or } C$ , and  $t_j = j\tau_{\text{vib}}$ . The Dirac bra-kets on the right-hand side of Eq. (10) are understood to be integrations over  $R_1$  and  $R_2$  that are limited in range to region D. The terms in the sum in Eq. (10) keep a quantum mechanically correct tabulation of probability lost due to absorption.

Consider a propagation of a metastable state corresponding to  $X_2BC(v')$ , and assume that asymptotic ( $t \rightarrow \infty$ ) product distributions have been estimated. A calculation with finite grids and absorption yields, in addition to finite  $P_v^P(\infty)$ , finite asymptotic probabilities  $P_v^C(\infty)$  associated with  $X + XBC(v)$ . This occurs because XBC lifetimes are typically twice as long as  $X_2BC$  lifetimes, i.e. in practical calculations some  $X + XBC$  density will be absorbed before it has had time to reach the  $2X + BC$  limit. If a hypothetical infinite time calculation could be performed with infinite grids, and no absorption in the  $X + XBC$  channels, then all amplitude will eventually go into some appropriately extended form of region P, because XBC is not stable for the accessible vibrational states. Let  $P_v$  be the "true" asymptotic probabilities in region P associated with this hypothetical calculation. The calculated probabilities  $P_v^P(\infty)$  must be underestimates of the

$P_v$ , owing to the fact that the  $P_v^C(\infty)$  are non-zero. Wave packet density in region C corresponds to  $X + XBC(v)$ . Neglecting interference effects between the regions, reasonable estimates of the  $P_v$  can be made on the basis of the dynamical properties of  $XBC(v) \rightarrow X + BC$ . Consider wave packet density in region C corresponding to  $X + XBC(v = v')$ . Actually, due to the relatively narrow energetic spreads of the wave packets and energy conservation arguments there is generally only a very small amount this. Suppose one could estimate the fraction  $Q_v^C$  of this density associated with quasibound  $XBC(v')$  complexes, i.e. complexes also associated with quantized vdW stretching motion. Separate 2D quantum calculations have been performed to show that all possible  $v'$  quasibound triatomic complexes decay predominantly (with probabilities  $> 90\%$ ) to  $X + BC(v'-1)$ . Thus  $Q_v^C P_v^C(\infty)$  is a contribution to  $P_{v'-1}$ . The remaining  $(1 - Q_v^C)$  fraction in the  $v'$  channel can be associated with direct scattering, i.e. processes that do not change  $v$  and lead to  $X + BC(v')$ . Thus,  $(1 - Q_v^C) P_v^C(\infty)$  represents a contribution to  $P_{v'-1}$ . The above arguments may be repeated for wave packet density in region C corresponding to  $XBC(v'-1)$  and  $XBC(v'-2)$ . Assuming the wave packet is expanded in terms of just three vibrational states ( $v', v'-1, v'-2$ ) one then has the following estimates for  $P_v$ :

$$\begin{aligned} P_{v'} &= P_{v'}^P(\infty) + (1 - Q_{v'}^C) P_{v'}^C(\infty) \\ P_{v'-1} &= P_{v'-1}^P(\infty) + Q_{v'}^C P_{v'}^C(\infty) + (1 - Q_{v'-1}^C) P_{v'-1}^C(\infty) \\ P_{v'-2} &= P_{v'-2}^P(\infty) + Q_{v'-1}^C P_{v'-1}^C(\infty) + (1 - Q_{v'-2}^C) P_{v'-2}^C(\infty) \\ P_{v'-3} &= Q_{v'-2}^C P_{v'-2}^C(\infty). \end{aligned} \quad (11)$$

Notice this procedure provides an estimate of probability associated with the  $v'-3$  channel, although this channel is not explicitly included in the propagation imagined. A straightforward generalization of Eq. (11) is used for calculations that explicitly include four vibrational states in the wave packet expansion.

The  $Q_v^C$  can be estimated by carrying out metastable state calculations on the 2D T-shaped problem, obtaining the various triatomic metastable states and then projecting them onto the wave packet near region C. For our purposes, the

triatomic metastable states may adequately be approximated by  $\psi_s(\mathbf{R})\chi_v(r)$ , where  $\{\psi_s(\mathbf{R}), s = 0, 1, \dots\}$  is a (finite) set of Morse oscillator functions corresponding to a Morse oscillator fit to the triatomic T-shaped potential for XBC. Let  $\Psi_v(\mathbf{R}_1, \mathbf{R}_2)$  denote a normalized cut of the full wave packet corresponding to vibrational component  $v$  near region C. For example, at some suitable time  $t$ ,  $C_v(\mathbf{R}_1, \mathbf{R}_2, t)$ , with  $\mathbf{R}_1$  between  $\mathbf{R}_C$  and  $\mathbf{R}_A$ , and  $\mathbf{R}_2$  between  $\mathbf{R}_0$  and  $\mathbf{R}_C$ , could be taken as being proportionate to  $\Psi_v(\mathbf{R}_1, \mathbf{R}_2)$ . Then

$$Q_v^C \approx \sum_s \int_{\mathbf{R}_C}^{\mathbf{R}_A} d\mathbf{R}_1 \left| \int_{\mathbf{R}_0}^{\mathbf{R}_C} d\mathbf{R}_2 \psi_s(\mathbf{R}_2) \Psi_v(\mathbf{R}_1, \mathbf{R}_2) \right|^2. \quad (12)$$

Since my concern is with obtaining rough (e.g., within  $\pm 10\%$ ) estimates of the product distributions, the approximate approach outlined has proven to be satisfactory.<sup>18</sup>

An additional difficulty in estimating the product distributions is encountered for cases with long lifetimes owing to computational difficulties in propagating the wave packets to an effective  $t \rightarrow \infty$  limit. One can, however, take advantage of the fact that, as in XBC vdW systems,<sup>6</sup> it is essentially short-time dynamics that determines the form of the product distributions. This is easily seen in practice by noting that the re-normalized asymptotic region probabilities for regions P and C,  $P_v^P(t)/N(t)$  and  $P_v^C(t)/N(t)$  with  $N(t) = \sum_v [P_v^P(t) + P_v^C(t)]$ , converge to at least two significant figures by times significantly less than the lifetime, e.g., typically by one quarter of the lifetime.

### 3. RESULTS

#### 3.1 He<sub>2</sub>Cl<sub>2</sub> and Ne<sub>2</sub>Cl<sub>2</sub>

Le Quere and Gray<sup>18</sup> have carried out extensive calculations for the He<sub>2</sub>Cl<sub>2</sub> and Ne<sub>2</sub>Cl<sub>2</sub> systems in the vibrational excitation range  $7 \leq v' \leq 13$  with the model outlined above. I will therefore discuss just a few representative results. Table 2. lists resonance properties and product distributions for several  $v'$  excitations in He<sub>2</sub>Cl<sub>2</sub>. Rather than report the resonance energies  $E_{res}$ , Table 2 displays the vdW bond energy  $D_0 = E_{v'} - E_{res}$ , where  $E_{v'}$  is the energy of an isolated BC( $v'$ ) molecule.

Table 2. Wave packet results for He<sub>2</sub>Cl<sub>2</sub>( $v'$ )

$v'$	$D_0 / \text{cm}^{-1}$	$\tau_{res} / \text{ps}^{-1}$	$P_v : v'-1$	$v'-2$	$v'-3$
8	32.5	45.0	0.04 [0.08]	0.91 [0.92]	0.02
10	32.5	22.6	0.04	0.90	0.03
12	32.4	11.9	0.04	0.89	0.05

(a) Results in square brackets correspond to experimental estimates from Ref. [10].  
(Due to energetic spreads in the wave packets, there is also a small probability of forming  $v'$  products, which I do not list.)

$D_0$  is the energy required to break both vdW bonds. Unfortunately, there is no experimental information available for either  $D_0$  or the lifetimes. Since the amount of energy available from just a one vibrational quantum change in BC,  $E_{v'} - E_{v'-1} \approx 140 \text{ cm}^{-1}$ , there is more than enough energy to break both bonds and thus form  $v_f = v'-1$  products. However, Table 2 shows that  $\approx 90\%$  of the products correspond to a two quantum change in BC. These results are thus consistent with experiment.<sup>10</sup> One may analyze the contributions to  $P_{v'-2}$  in Eq. (11) and deduce that the  $Q_{v'-1}^C P_{v'-1}^C(\infty)$  term is

largely responsible for the large magnitudes of  $v'-2$  products, which points to the sequential mechanism Eq. (2) being dominant.

Inspection of the wave packet also shows this clearly, i.e. one sees almost no wave packet amplitude associated with a direct fragmentation process. For example, Fig. 3 below displays contours of the reduced wave packet density

$$\rho(R_1, R_2, t) = \int dr |\Psi(R_1, R_2, r, t)|^2, \quad (13)$$

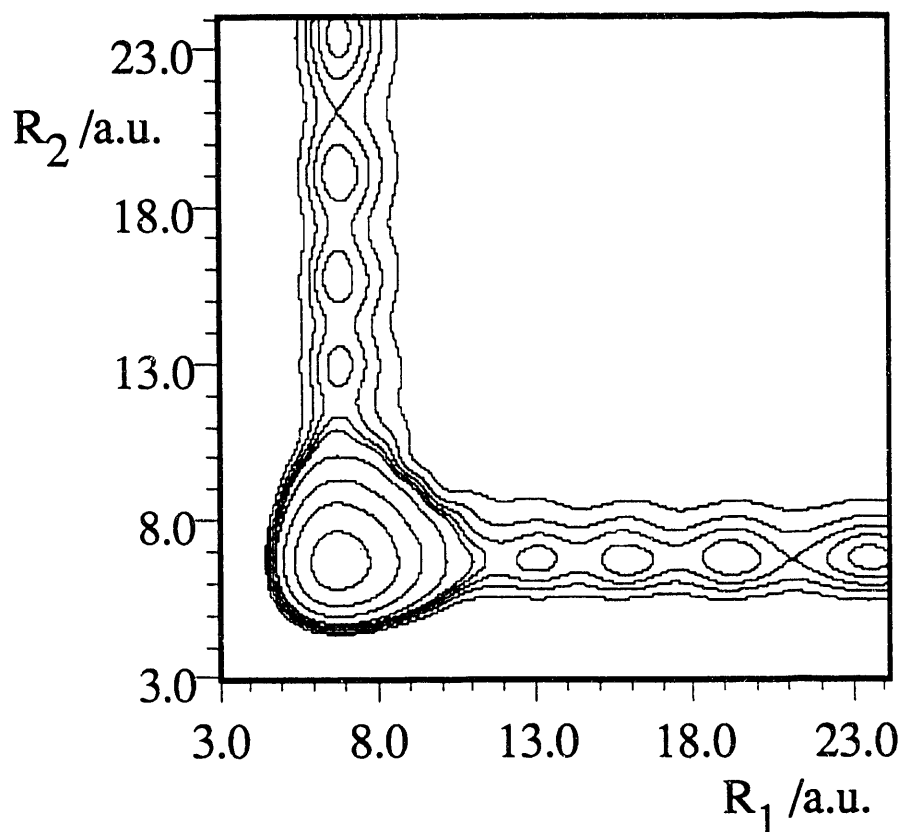


Fig. 3. Contours of the reduced density for  $\text{He}_2\text{Cl}_2(v'=12)$  at  $t = 2$  ps.

at  $t \approx 2$  ps for the  $v' = 12$  propagation. Wave packet density is strongly peaked in the interaction region consistent with the initially prepared  $\text{He}_2\text{Cl}_2(v'=12)$  metastable state. Contour levels corresponding to small amounts of wave packet density are evident in the two  $X + \text{XBC}$  channels. There is some density in the  $2X + \text{BC}$  limit as well, although it is quite small (less than one percent of the total density) at this time. It is possible to analyze the density and discover that almost all density in the  $X + \text{XBC}$  channels corresponds to  $\text{XBC}(v'-1)$  triatomic metastable states with zero-point energy in the vdW stretch. These states (eventually) decay with almost unit probability to  $v'-2$  states and so Fig. 3 is the quantum mechanical representation of the sequential dynamics mechanism Eq. (2).

Table 3 presents some results obtained for  $\text{Ne}_2\text{Cl}_2$ , and contrasts them with available experimental information. The vdW bond energy and lifetimes are in surprisingly good accord with experiment, given the obvious limitations of the model. The product distributions for  $v' = 10$  and  $12$  are also in good accord with experiment. However, in this case it is clear that the vdW bond energy is such that the  $v'-1$  product channel is closed for  $v' \geq 10$ . This means that if energy-resolved probabilities were determined corresponding to the resonance energy, there would be no probability of forming  $v'-1$  products. There is a small amount of  $v'-1$  probability in Table 3 only because the wave packets have a small energetic spread. Therefore, the fact that  $v'-2$  products dominate for  $v' = 10$  and  $12$  is not too surprising. In this regime, there is also good agreement with experiment. However, the  $v' = 8$  product distribution inferred from the model is very similar to the  $v'$

= 10 and 12 results (and the He<sub>2</sub>Cl<sub>2</sub> results above). The model predicts a sequential mechanism is operative even when the v'-1 channel is open.

Table 3. Wave packet results for Ne<sub>2</sub>Cl<sub>2</sub>(v')<sup>(a)</sup>

v'	D <sub>0</sub> /cm <sup>-1</sup>	τ <sub>res</sub> /ps <sup>-1</sup>	P <sub>v</sub> :	v'-1	v'-2	v'-3
8	152	139 [124]		0.04 [0.5*]	0.91 [0.5*]	0.02 [0.0]
10	151	50 [62*]		0.04 [0.0]	0.90 [1.0]	0.03 [0.0]
12	151	19 [21*]		0.04 [0.0]	0.89 [1.0]	0.05 [0.0]

(a) Results in square brackets correspond to experimental estimates from Ref. [11]. An asterisk (\*) indicates that I interpolated the result on the basis of the data in Ref. [11]. An experimental estimate<sup>11</sup> of ≈ 147 cm<sup>-1</sup> has been reported for D<sub>0</sub>.

Experiment in this limit, however, yields a different result, with at v' = 8 roughly equal amounts of v'-1 and v'-2 being present. (The v' = 8 "experimental" distribution in Table 3 is an interpolation of results given in Ref. [11] for v' = 7 and 9.) Furthermore, if v' = 7 is considered (not shown in Table 3) one finds still ≈ 90 % of the products are predicted to be in v'-2 with the model, whereas experiment shows only ≈ 20% are in v'-2, with ≈ 80% being in v'-1 instead. The failure of the model for low levels of vibrational excitation in Ne<sub>2</sub>Cl<sub>2</sub> has been attributed to neglect of θ variation (see Fig. 1).<sup>18</sup> It was shown that just slightly smaller θ values than equilibrium can enhance the v'-1 product channel. This happens through increased Ne...Ne interactions and thus an enhancement of a direct fragmentation mechanism involving essentially a simultaneous departure of both Ne atoms with only a one quantum loss from Cl<sub>2</sub>. This effect is less important in He<sub>2</sub>Cl<sub>2</sub> because of the generally weaker He...He interactions (see Table 1).

### 3.2 He<sub>2</sub>I<sub>2</sub> and Ne<sub>2</sub>I<sub>2</sub>

I have just started to analyze these systems, and will outline here a few preliminary results. Wave packet calculations for He<sub>2</sub>I<sub>2</sub>(v'=22) have been performed. As with all previous X = He results, the dynamics was found to be sequential with P<sub>v'-1</sub> = 0.01, P<sub>v'-2</sub> = 0.93 and P<sub>v'-3</sub> = 0.06. These results compare surprisingly well with experimental results from Levi's group:<sup>8</sup> P<sub>v'-1</sub> = 0.015, P<sub>v'-2</sub> = 0.94, and P<sub>v'-3</sub> = 0.044! This excellent agreement must be a partly fortuitous but nonetheless is encouraging. The lifetime for He<sub>2</sub>I<sub>2</sub>(v'=22) was determined to be 19 ps. No experimental result is available for comparison. A calculation was performed for He<sub>2</sub>I<sub>2</sub>(v'=12), which led to a longer lifetime of 65 ps, but a similar product distribution.

The Ne<sub>2</sub>I<sub>2</sub>(v') system proved to be more interesting. A wave packet propagation of a Ne<sub>2</sub>I<sub>2</sub>(v'=21) initial state led to significant amounts of v<sub>F</sub> = v'-3 products. The largest vibrational state probabilities were estimated to be: P<sub>v'-2</sub> ≈ 0.1, P<sub>v'-3</sub> ≈ 0.8, and P<sub>v'-4</sub> ≈ 0.1. In a quantitative sense, these results do not compare favorably with experimental results from Levi's group<sup>9</sup> that indicate the v'-2 and v'-3 channels are about equally populated for v' = 21 predissociation: P<sub>v'-2</sub> = 0.55, P<sub>v'-3</sub> = 0.41 and P<sub>v'-4</sub> = 0.04. However, qualitatively the model is correctly predicting significant amounts of v'-3 products, which is inconsistent with the sequential mechanism Eq. (2) that might be expected to be operative. Another important feature (that may partly explain the quantitative discrepancies between theory and experiment) to note is that the dynamics is now *strongly* dependent on v'. A wave packet calculation for v' = 16 did yield v'-2 and v'-3 products in nearly a 50:50 ratio and a calculation for v' = 12 led to the old picture of sequential dynamics, with over 90% of the products being in v'-2. The trend towards a sequential mechanism with decreasing v' is also indicated by the (limited) available experimental data.<sup>9</sup> Therefore it may be that small variations in potential parameters and/or inclusion of certain zero-point effects due to bending motion may shift the theoretical results into better accord with experiment. I should also note that Levi's group determined a lifetime of 99 ps for the v' = 12 case, which compares well with my theoretical estimate of 90 ps based on Prony analysis of the v' = 12 correlation function.

What makes  $\text{Ne}_2\text{I}_2(v')$  behave so interestingly in the  $v' \approx 21$  range? Analysis of the wave packet correlation functions shows that the wave packets actually contain contributions from at least two resonances in this range. Plots of the vibrational state probabilities also show that the  $v'$  and  $v'-1$  total probabilities (i.e., summed over all regions D in Fig. 2) *oscillate* in a correlated manner. This all points to an IVR phenomenon, akin to that seen in  $\text{ArCl}_2$ <sup>6</sup> and  $\text{ArI}_2$ .<sup>7</sup> Individual resonances that normally contain zero-point motion in the vdW degrees of freedom and  $v'$  quanta of excitation in the BC part turn out to become more mixed when  $v' \approx 21$  and contain noticeable amounts of  $v'-1$  character too. This arises from certain zero-order degeneracies between excited vdW states in the  $v' - 1$  manifold and the usual metastable state corresponding to zero-point vdW excitation in the  $v'$  manifold. The result is at least two resonances that are close to one another in energy, with one being mostly (but not entirely)  $v'$  in character and another being mostly (but not entirely)  $v'-1$  in character. The initial metastable state, which is entirely  $v'$  in character, then overlaps with both resonances. Such accidental degeneracies will also be very sensitive to  $v'$ . Interestingly, recent real-time experiments from Zewail's group<sup>17</sup> have also pointed to such possibilities. They have suggested the potential importance of  $\text{Ne}_2\text{I}_2(v'-1)$  intermediates that contain significant amounts of vdW symmetric stretching excitation. Such intermediates (via a sequential mechanism like Eq. (2) but with all quantum numbers decreased by one) could yield the  $v'-3$  products. It should be possible to analyze the wave packets and ascertain the presence of intermediates of this type, and work is in progress along these lines. One aspect that is clear from my analysis so far is that most of the  $v'-3$  products do indeed arise from  $\text{Ne} + \text{NeI}_2(v'-2)$  type states, which is consistent with the IVR picture.

#### 4. CONCLUDING REMARKS

I have presented a three degrees of freedom model for  $\text{X}_2\text{BC}$  vibrational predissociation, and outlined how to perform wave packet calculations on this model. The results of Le Quere and Gray<sup>18</sup> on  $\text{He}_2\text{Cl}_2$  and  $\text{Ne}_2\text{Cl}_2$  were discussed, and I also presented some preliminary results for  $\text{He}_2\text{I}_2$  and  $\text{Ne}_2\text{I}_2$ .

Despite  $\text{He}_2\text{BC}$  molecules being very floppy, their vibrational predissociation dynamics is adequately described by the simple model that freezes the angle between  $\theta$  the two helium atoms and the center of mass of BC. A sequential fragmentation mechanism is always operative. The relative weakness of He...He potential interactions is responsible for these features.

$\text{Ne}_2\text{BC}$  systems offer a more complex dynamics experimentally. The  $\text{Ne}_2\text{Cl}_2$  theoretical model results were not an adequate description of the low  $v'$  excitation ( $v' < 10$ ) experimental dynamics, although the  $v' \geq 10$  dynamics was properly described. The model severely underestimated the amount of  $v'-1$  products consistent with a direct fragmentation of both Ne atoms in the low  $v'$  limit. Le Quere and Gray<sup>18</sup> have shown that small variations in  $\theta$  can lead to increased Ne...Ne interactions and an enhancement of the direct mechanism product  $v'-1$  channel. Clearly, these results suggest a four dimensional model, explicitly including  $\theta$  as a dynamical variable should be developed and studied.

The  $\text{Ne}_2\text{I}_2$  results were interesting because of the occurrence of IVR resonances near  $v' \approx 21$ . It is necessary to characterize these resonances in greater detail, and work is in progress towards this end. The classical analogue of the IVR resonances is a nonlinear classical resonance zone in phase space,<sup>20</sup> so classical trajectory studies may also prove to be interesting. It may also be possible to find these resonances in  $\text{Ne}_2\text{Cl}_2$ , but at slightly higher vibrational excitations than those studied here and in the experiments.<sup>11</sup> Some preliminary calculations, in fact, suggest that similar resonances can occur in  $\text{Ne}_2\text{Cl}_2$  when  $v' \approx 15$ .

#### 5. ACKNOWLEDGMENTS

This research was supported by the Office of Basic Energy Services, Division of Chemical Science, US Department of Energy under Contract No. W-31-109-ENG-38. I also thank George Schatz for making several useful comments on this project.

## 6. REFERENCES

1. J.A. Beswick and J. Jortner, "Intramolecular dynamics of van der Waals molecules," *Adv. Chem. Phys.*, Vol. 47, pp. 363-506, 1981, and references therein.
2. J.I. Cline, B.P. Reid, D.D. Evard, N. Sivakumar, N. Halberstadt, and K.C. Janda, "State-to-state vibrational predissociation and spectroscopy of  $\text{HeCl}_2$ : Experiment and theory," *J. Chem. Phys.*, Vol. 89, pp. 3535-3552, 1988.
3. J.I. Cline, N. Sivakumar, D.D. Evard, C.R. Bieler, B.P. Reid, N. Halberstadt, and K.C. Janda, "Product state distribution for the vibrational predissociation of  $\text{NeCl}_2$ ," *J. Chem. Phys.*, Vol. 90, pp. 2605-2616, 1989.
4. D.M. Willberg, M. Gutmann, J.J. Breen, and A.H. Zewail, "Real-time dynamics of clusters. I.  $\text{I}_2\text{X}_n(n=1)$ ," *J. Chem. Phys.*, Vol. 96, pp. 198-212, 1992.
5. S.K. Gray and C.E. Wozny, "Fragmentation mechanisms from three-dimensional wave packet studies: Vibrational predissociation of  $\text{NeCl}_2$ ,  $\text{HeCl}_2$ ,  $\text{NeCl}$  and  $\text{HeCl}$ ," *J. Chem. Phys.*, Vol. 94, pp. 2817-2832, 1991.
6. N. Halberstadt, J.A. Beswick, O. Roncero, and K.C. Janda, "Intramolecular vibrational relaxation in a triatomic van der Waals molecule:  $\text{ArCl}_2$ ," *J. Chem. Phys.*, Vol. 96, 2404-2407, 1992.
7. S.K. Gray, "Quantum dynamics of  $\text{ArI}_2 \rightarrow \text{Ar} + \text{I}_2$ ," *Chem. Phys. Lett.*, Vol. 197, pp. 86-91, 1992.
8. W. Sharfin, K.E. Johnson, L. Wharton, and D.H. Levy, "Energy distribution in the photodissociation products of van der Waals molecules: Iodine-helium complexes," *J. Chem. Phys.*, Vol. 71, pp. 1292-1299, 1979.
9. J.E. Kenny, K.E. Johnson, W. Sharfin, and D.H. Levy, "The photodissociation of van der Waals molecules: Complexes of iodine, neon, and helium," *J. Chem. Phys.*, Vol. 72, pp. 1109-1119, 1980.
10. W.D. Sands, C.R. Bieler, and K.C. Janda, "Spectroscopy and dynamics of  $\text{He}_2\text{Cl}_2$ : A quantum liquid cluster?" *J. Chem. Phys.*, Vol. 95, pp. 729-734, 1991.
11. S.R. Hair, J.I. Cline, C.R. Bieler, and K.C. Janda, "The structure and dynamics of the  $\text{Ne}_2\text{Cl}_2$  van der Waals complex," *J. Chem. Phys.* Vol. 90, pp. 2935-2943, 1989.
12. G.C. Schatz, V. Buch, M.A. Ratner, and R.B. Gerber, "Dissociation dynamics of vibrationally excited van der Waals clusters:  $\text{I}_2\text{XY} \rightarrow \text{I}_2 + \text{X} + \text{Y}$ ," *J. Chem. Phys.*, Vol. 79, pp. 1808-1821, 1983.
13. A. Garcia-Vela, P. Villarreal, and G. Delgado-Barrio, "An approximate quantal treatment to obtain the energy levels of tetra-atomic  $\text{X} \dots \text{I}_2 \dots \text{Y}$  van der Waals clusters," *J. Chem. Phys.*, Vol. 92, pp. 496-507, 1990.
14. A. Garcia-Vela, P. Villarreal, and G. Delgado-Barrio, "Structure and dynamics of small  $\text{I}_2 \dots \text{He}_n$  van der Waals clusters," *J. Chem. Phys.*, Vol. 92, pp. 6504-6513, 1990.
15. A. Garcia-Vela, P. Villarreal, and G. Delgado-Barrio, "Dissociation dynamics of  $\text{I}_2 \dots \text{Ne}_n$  van der Waals clusters ( $n=1-9$ ): A quasiclassical approach," *J. Chem. Phys.*, Vol. 94, pp. 7868-7874, 1991.
16. Z. Bacic, M. Kennedy-Mandziuk, J.W. Moskowitz, and K.E. Schmidt, " $\text{He}_2\text{Cl}_2$  and  $\text{He}_3\text{Cl}_2$  van der Waals clusters: A quantum Monte Carlo Study," *J. Chem. Phys.*, Vol. 97, pp. 6472-6482, 1992.
17. M. Gutmann, D.M. Willberg, and A.H. Zewail, "Real-time dynamics of clusters: III.  $\text{I}_2\text{Ne}_n$  ( $n=2-4$ ), picosecond fragmentation and evaporation," *J. Chem. Phys.*, submitted, 1992.
18. F. Le Quere and S.K. Gray, "Quantum dynamics of van der Waals clusters: Model results for  $\text{He}_2\text{Cl}_2$  and  $\text{Ne}_2\text{Cl}_2$  fragmentation," *J. Chem. Phys.*, submitted, 1992.
19. See, e.g., B.R. Johnson and W.P. Reinhardt, "Adiabatic separations of stretching and bending vibrations: Application to  $\text{H}_2\text{O}$ ," *J. Chem. Phys.*, pp. 4538-4556, 1986.
20. S.K. Gray, S.A. Rice, and D.W. Noid, "The classical mechanics of vibrational predissociation: A model based study of phase space structure and its influence on fragmentation rates," *J. Chem. Phys.*, Vol. 84, pp. 3745-3752, 1986.
21. S.K. Gray, "Wave packet dynamics of resonance decay: An iterative equation approach with application to  $\text{HCO} \rightarrow \text{H} + \text{CO}$ ," *J. Chem. Phys.*, Vol. 96, pp. 6543-6554, 1992.
22. P. Pernot and W.A. Lester, Jr. "Multidimensional wave-packet analysis: Splitting method for time-resolved property determination," *Int. J. Quant. Chem.*, Vol. 40, pp. 577-588, 1991.

## DISCLAIMER

This report was prepared as an account of work sponsored by an agency of the United States Government. Neither the United States Government nor any agency thereof, nor any of their employees, makes any warranty, express or implied, or assumes any legal liability or responsibility for the accuracy, completeness, or usefulness of any information, apparatus, product, or process disclosed, or represents that its use would not infringe privately owned rights. Reference herein to any specific commercial product, process, or service by trade name, trademark, manufacturer, or otherwise does not necessarily constitute or imply its endorsement, recommendation, or favoring by the United States Government or any agency thereof. The views and opinions of authors expressed herein do not necessarily state or reflect those of the United States Government or any agency thereof.

**END**

---

**DATE  
FILMED**

**5 / 7 / 93**